Finest light curve details, physical parameters, and period fluctuations of CoRoT[*] RR Lyrae stars

J. M. Benkő,[1]† R. Szabó,[1] A. Derekas[2,1] and Á. Sódor[1]

[1] *Konkoly Observatory, MTA CSFK, Konkoly Thege M. u. 15-17., H-1121 Budapest, Hungary*
[2] *ELTE Gothard Astrophysical Observatory, Szent Imre herceg út 112., H-9704 Szombathely, Hungary*

ABSTRACT

The CoRoT satellite supplied the scientific community with a huge data base of variable stars. Among them the RR Lyrae stars have intensively been discussed in numerous papers in the last few years, but the latest runs have not been checked to find RR Lyrae stars up to now. Our main goal was to fill this gap and complete the CoRoT RR Lyrae sample. We found nine unstudied RR Lyrae stars. Seven of them are new discoveries. We identified three new Blazhko stars. The Blazhko effect shows non-strictly repetitive nature for all stars. The frequency spectrum of the Blazhko star CoRoT 104948132 contains second overtone frequency with the highest known period ratio. The harmonic amplitude and phase declines with the harmonic order were studied for non-Blazhko stars. We found a period dependent but similar shape amplitude decline for all stars. We discovered significant random period fluctuation for one of the two oversampled target, CM Ori. After a successful transformation of the CoRoT band parameters to the Johnson V values we estimated the basic physical properties such as mass, luminosity, metallicity. The sample can be divided into two subgroups with respect to the metallicity but otherwise the physical parameters are in the canonical range of RR Lyrae stars.

Key words: Stars: variables: RR Lyrae – stars: oscillations – stars: interiors – techniques: photometric – space vehicles

1 INTRODUCTION

The recent photometric space missions such as CoRoT (Baglin et al. 2006) and *Kepler* (Borucki et al. 2010) yielded long and quasi-uninterrupted time series with high precision for a huge amount of variable stars. Although few people expected previously, many amazing discoveries have been made for classic high amplitude variables stars, as RR Lyraes. Among others these mission revealed the excitation of low amplitude modes for many Blazhko RRab stars, one of which is responsible for the so-called period doubling phenomenon (Kolenberg et al. 2010; Szabó et al. 2010; Kollath et al. 2011), while others show the famous ~0.61 period ratio of the RRc stars (Moskalik et al. 2015) or just appear as an additional mode(s) resulting in non-traditional double and triple mode stars (Benkő et al. 2010).

The CoRoT satellite was one of the most successful in

these discoveries. Up to now about ten peer-reviewed scientific articles published CoRoT RR Lyrae results. The paper of Szabó et al. (2014) gives a good overview of these. Previous works discussed 13 stars observed in long runs only and till the end of the fourth long run towards the Galactic center direction (LRc04). Neither the short nor the late runs were investigated for searching RR Lyrae stars. We make up for this incompleteness with the present work.

2 SAMPLE SELECTION

Since hundreds of papers appeared on the basis of the CoRoT satellite data the basic facts about the satellite and its equipment are well-known, we only refer here the most important instrumental paper (Auvergne et al. 2009) and on-line documentations[1] where the reader can find the details of the mission. This work used the CoRoT Public Archive N2 data of Exo-fields. For simplicity, we used the entire data base in our RR Lyrae search including the initial run (IRa01), long runs (LRa01-LRa07, LRc01-LRc10), and

---

[1] `http://idoc-corot.ias.u-psud.fr/sitools/client-user/COROT_N2_PUBLIC`

Table 1. Some parameters of the discussed CoRoT archive RR Lyrae stars. The columns contain the CoRoT ID, variable name (if exists), the brightness (specified by the Exo-Dat Catalogue Deleuil et al. 2009), position (RA, DEC), pulsation period P_0, Fourier amplitude of the main pulsation frequency $A(f_0)$, Blazhko period P_B, observed time span Δt in days, and CoRoT run identifier, respectively. Last three digits of the CoRoT numbers are boldfaced. We refer to the stars by these short numbers instead of the complete IDs.

Corot ID	Name	m_{EXO} [mag]	RA hh:mm:ss.ss	DEC d:mm:ss.s	P_0 [d]	$A(f_0)$ [mag]	P_B [d]	Δt [d]	Run ID
102326**020**		14.654	06:10:59.87	4:40:32.5	0.77029	0.1296	79.5	148.31	LRa03
104948**132**		15.217	18:37:43.63	4:01:44.2	0.58642	0.2420	28.1	87.26	LRc05
205924**190**		13.600	18:57:17.45	−4:16:39.4	0.72049	0.1053		20.86	SRc02
605307**902**		15.170	06:08:42.38	6:22:15.1	0.62418	0.1559		77.6	LRa04
617282**043**	CM Ori	12.889	06:03:54.87	8:14:32.4	0.65593	0.2859		90.48	LRa05
651349**561**		14.708	19:14:03.69	−2:27:54.8	0.61179	0.1013	21.9	83.51	LRc09
655183**353**		14.911	19:14:41.21	−2:06:09.1	0.69426	0.1921		83.51	LRc09
657944**259**		14.954	19:18:08.54	−2:34:43.9	0.57787	0.1876		83.51	LRc09
659723**739**	V2042 Oph	15.186	18:32:46.97	7:58:05.7	0.53849	0.2761		81.22+83.47	LRc07+LRc10

short runs (SRa01-SRa05, SRc01-SRc03). Here the letters 'c' and 'a' denote that the CoRoT observed either toward the Galactic centre or anti-centre directions, respectively. The advantage of the use of the total observing material is that we can check our search efficiency when we compare our candidates in the early runs with the RR Lyraes found by former studies.

We used the automatic CoRoT Variable Classifier (CVC; Debosscher et al. 2009) when we searched for RR Lyrae stars separately for each subtype in the complete data base. The CVC has improved a lot since the beginning. Our present search results illustrate this well: if we decrease the probability level assigned by CVC of RRab stars from >50% to >10%, then to >0%, we found 15, 16 and 18 candidates, respectively. Investigating the candidates by visual inspection only one of them proved to be non-RR Lyrae stars in the lowest probability group. All others (17) show clear RR Lyr light curve properties. Eight RRab stars were discussed by former studies (Szabó et al. 2014, and references therein). Two additional RRab stars were known in the CoRoT sample (CoRoT 101315488 and CoRoT 100881648) which have not been found by CVC. These stars are, however, heavily blended by nearby stars and therefore their variability have much smaller amplitude and distorted light curves compared to a normal RR Lyrae star. The CoRoT data of nine RRab stars have not been discussed anywhere yet. These stars constitute the present sample (see Table 1). Fig. 1 shows small light curve parts of each star. The RR Lyrae nature of two stars: CM Ori (CoRoT 617282043) and V2042 Oph (CoRoT 659723739) have already been known but the other seven ones are completely new discoveries.

The same process (CVC with decreasing probability levels and visual light curve examination) has been carried out for RRc subtype as well. For RRc stars we get 25, 34 and 137 candidates for >50%, >10%, and >0% probability levels, respectively. The two known RRc stars (CoRoT 105036241 and CoRoT 105735652) were already contained in the highest probability group. The increasing candidate numbers of the lower probability level groups did not result in new RRc stars. The groups consist mostly of binary stars and some spotted and HADS/SX Phe candidates.

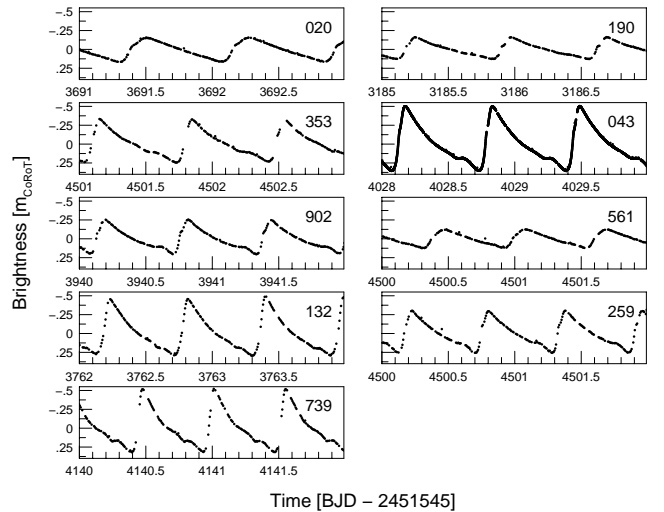In the case of double mode RR Lyrae stars (RRd) the CVC yields different kind of results. For >50%

Figure 1. Light curve zoo of the CoRoT RR Lyrae stars found by this work. The time and brightness scales are uniform for all panels. The panels are ordered from top left to bottom right by the decreasing pulsation period.

and >10% probability levels we get only one candidate (CoRoT 101368812) which is known as a bona fide RRd star (Chadid 2012), while for >0% probability level the number of candidates abruptly increases to 7650. We applied a semi-automatic method to handle this large number of light curves. We calculated the Fourier amplitude spectra in the $1-10\,d^{-1}$ range of all the 7650 light curves. We selected all peaks from these spectra that exceeded the 4σ amplitude, where σ was calculated as the $3\,d^{-1}$ moving average of the amplitude spectrum. The classical double mode RR Lyrae stars have a well-known period ratio between their radial fundamental and first overtone modes $P_1/P_0 \sim 0.72$-$0.755\,d^{-1}$ which defines the Petersen diagram (see e.g. in Soszyński et al. 2014). Therefore, we selected those objects that have their highest peak f_{max} in the $1-5\,d^{-1}$ range and that have at least one further significant peak in either the $0.72f_{max}-0.755f_{max}$ or the $f_{max}/0.755-f_{max}/0.72$ range. These are those stars that have frequency ratio in the
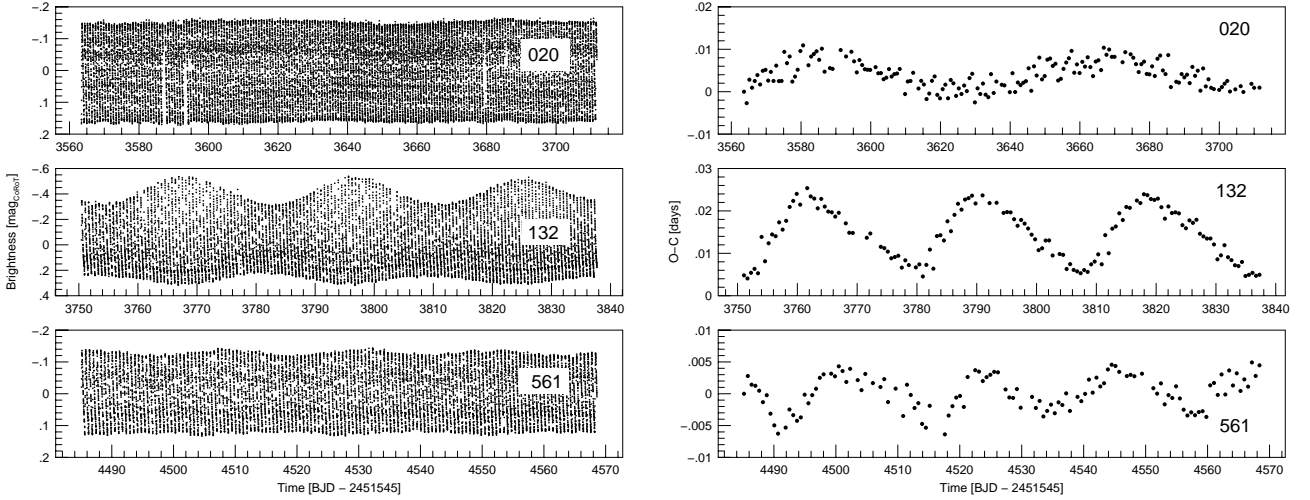
Figure 2. Complete CoRoT observations of the new Blazhko stars (on the left) and their O-C diagrams (on the right).

0.72 – 0.755 range with the largest-amplitude peak. This selection yielded 113 objects. We investigated the light curves and Fourier spectra of these 113 objects visually. Apart from the known CoRoT 101368812, we did not find any further RRd pulsator. Note that 61 targets were identified as γ Dor candidates and 42 as eclipsing/heartbeat binary candidates.

From now on, this paper refers CoRoT stars with the last three digits (boldfaced in the first column in Table 1) of their ID number for short notation.

3   TIME SERIES ANALYSIS

After we extracted the downloaded data files we applied trend and jump filtering, outlier removal, and a transformation into the magnitude scale as we described in detail in Chadid et al. (2010)[2]. Two of our targets (CM Ori and #190) were bright enough to be observed by CoRoT in colour mode, but because of the uniform handling, we also used their integrated (white light) fluxes only. The nominal sampling is 512 sec for all the stars, except CM Ori, where the the light curve was observed with the much denser oversampling mode (32 sec). The data set of CM Ori is twice as dense as the *Kepler*/K2 short cadence observations.

The main tool was a standard discrete Fourier analyzer implemented by the program package MuFrAn (Kolláth 1990). It yields sinusoidal Fourier decomposition, therefore, we used this one through this paper. The Nyquist frequency of the normal and oversampled data are 84.375 d^{-1}, and 1350 d^{-1}, respectively. The stability of the periods were checked by O−C diagrams (Sterken 2005). The O−C diagrams were constructed from the maximum brightness times. The proper maximum times were determined by light curve maxima with 7-10 order polynomial fits.

The Fourier spectra of the analyzed nine stars are dominated by the main pulsation frequencies and their harmonics. Simultaneous non-linear fits to the light curves with
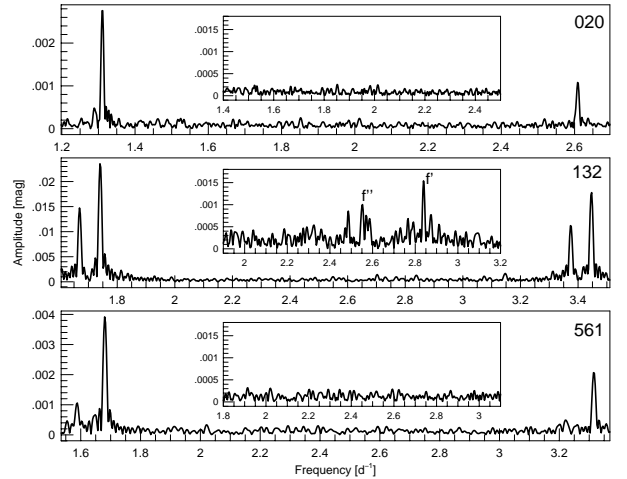
Figure 3. Fourier spectra of the Blazhko stars on the interval $(f_0 - 0.1, 2f_0 + 0.1)$, after we pre-whitened the data with f_0 and all significant harmonic frequencies. The inserts show narrower ranges $(f_0 + 0.1, 2f_0 - 0.1)$ of the spectra after a further pre-whitening step in which we removed all the significant modulation side frequencies as well.

these frequencies resulted in the pulsation periods P_0 and the amplitudes $A(f_0)$ given in Table 1.

3.1   Blazhko stars

#020: The light curve shows a slight amplitude change (see the top left panel in Fig. 2). After we pre-whitened the data with the main pulsation frequency and its significant harmonics we found significant peaks in the residual spectrum around the pre-whitened frequency positions. We can identify them as Blazhko modulation frequencies as $if_0 \pm f_B$, (i is positive integer). The Blazhko period P_B given in Table 1 was calculated from the average of the side peak differences around the main peak. The side peak amplitudes are highly asymmetric, the right hand side peaks are much higher than the left hand side ones (see the top panel in

Fig. 3). This asymmetry, however, decreases with the increasing harmonic order: while the $f_0 - f_B$ and $f_0 - 2f_B$ are around the detection limit, $f_0 - 3f_B$ and even $f_0 - 4f_B$ are much less asymmetric. This behaviour has a natural explanation in the simultaneous amplitude and frequency modulation framework (Benkő et al. 2011). In the O−C diagram (top right in Fig. 2) we indeed find a periodic signal with 80.7 d^{-1} period and ∼5 min amplitude which can be identified as the frequency modulation part of the Blazhko effect.

The pulsation period of the star #020 is one of the longest ($P_0 = 0.77029$ d) ever found for a Blazhko RR Lyrae star. Its Blazhko period is long enough to test the relation between the pulsation period and Blazhko period discovered by Jurcsik et al. (2005a). They found that the Blazhko frequency, which was represented by the frequency separation between the main pulsation frequency and the side frequencies, has a maximal allowed value at a given pulsation frequency. These maximal values form a linear upper envelope curve in the pulsation frequency vs. Blazhko frequency diagram (see fig. 6 in Jurcsik et al. 2005a). The position of #020 is under this upper envelope line supporting the finding of the paper. Both the amplitude and frequency modulation parts of the two observed Blazhko cycles differ from each other (top panels in Fig. 2). This raises the possibility of multiperiodic (or chaotic) nature of the modulation, but such a short observing span does not allow us to confirm or reject these hypotheses.

#132: The light curve in the middle left panel in Fig. 2 shows three clear Blazhko cycles with decreasing amplitudes. The Fourier spectrum contains evident triplet structures around the main pulsation frequency and all its harmonics. The low-frequency range of the spectrum contains three significant frequencies: $f^{(1)} = 0.0355$ d^{-1}, $f^{(2)} = 0.0143$ d^{-1} and $f^{(3)} = 0.0475$ d$^{-1} \approx f^{(1)} + f^{(2)}$. The frequency $f^{(1)}$ can be interpreted as the Blazhko frequency f_B itself, the $f^{(2)}$ most probable belongs to the total time span, and $f^{(3)}$ is a linear combination of these two frequencies. After the first two pre-whitening steps in which we removed the main pulsation frequency, its harmonics and all significant Blazhko side peaks the residual spectrum shows two groups of significant peaks between the harmonics (middle panel in Fig. 3). These peaks are most robust between the main pulsation frequency and the first harmonic. The highest peak is at $f' = 2.8394$ d^{-1} while the second one is at $f'' = 2.5519$ d^{-1}. The latter frequency can be identified as $f'' \approx 3/2 f_0$ which belongs to the period doubling phenomenon. What about the frequency f'? Numerous studies (Benkő et al. 2010, 2014; Poretti et al. 2010; Szabó et al. 2014; Molnár et al. 2015) found frequencies at this position: between the period doubling (PD) frequencies and the first overtone. These frequencies are explained by the f_2 second radial overtone mode or a non-radial mode which is excited close to the position of the second overtone mode. #132 has the highest period ratio $P_2/P_0 = 0.601$ ever detected.

The identification of the $f' = f_2$ is verified with theoretical model calculations. Fig. 4 shows a theoretical Petersen diagram where the periods P_0, P_1, P_2, P_3, P_4 belong to the radial fundamental, first, second, third and fourth overtone modes, respectively. The different metallicity models are noted by different symbols. The parameters and details of the models are the same as it was described in Chadid et al. (2010). As we see the ratio of f' is
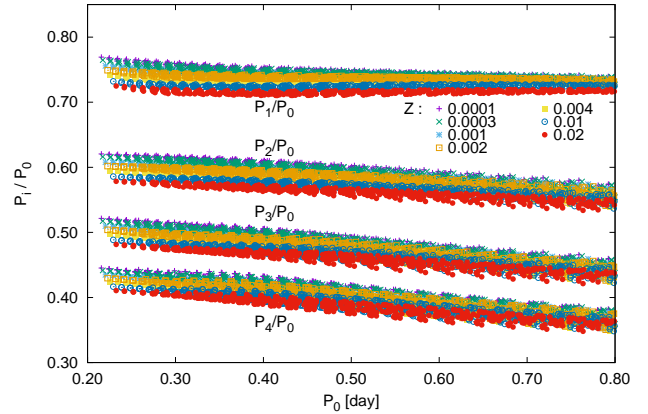

Figure 4. Theoretical Petersen diagram based on linear convective RR Lyrae models up to the 4th radial overtone modes. The symbols denote different metallicities.

in the allowed range of second overtone frequencies. That is the Fourier spectrum of #132 shows the PD and the radial second overtone mode frequencies simultaneously similarly to some other stars in the CoRoT and *Kepler* samples (e.g. CoRoT 101128793 Poretti et al. 2010; V355 Lyr, KIC 7257008, and KIC 9973633 Benkő et al. 2014).

The O−C diagram in the middle right panel in Fig. 2 shows evident frequency modulation. The Fourier spectrum of the O−C diagram contains f_B and $2f_B$ reflecting the non-sinusoidal nature of the variation. The consecutive Blazhko cycles are different but do not show declining amplitudes as opposed to the light curve. The strictly mono-periodic nature of the Blazhko effect, similarly to the case of the star #020, can be ruled out both on the basis of the light and O−C curves.

#561: Both the light and O−C curves (bottom panels in Fig. 2) show the Blazhko effect. The amplitude modulation seems to be more regular than the frequency modulation part. The modulation side peaks in the Fourier spectrum of the light curve are asymmetric: left hand side peaks have lower amplitudes than the right hand side ones. After we removed all the significant side frequencies, no additional frequencies have been found in the residual spectrum. Interestingly, while all stars that show additional frequencies show the Blazhko effect as well (Benkő & Szabó 2015), the reverse statement is not true. There are known some CoRoT (Szabó et al. 2014) and *Kepler*/K2 (Benkő et al. 2014; Molnár et al. 2015) Blazhko stars without any additional frequencies. As we show here the stars #561 and #020 seem to belong to this group. We can speculate whether this finding is a selection effect or a real feature. The selection effect explanation is supported by the time dependence of these additional frequencies. They have low and highly time dependent amplitude. So these frequencies could disappear from the frequency content for a while and then emerge again.
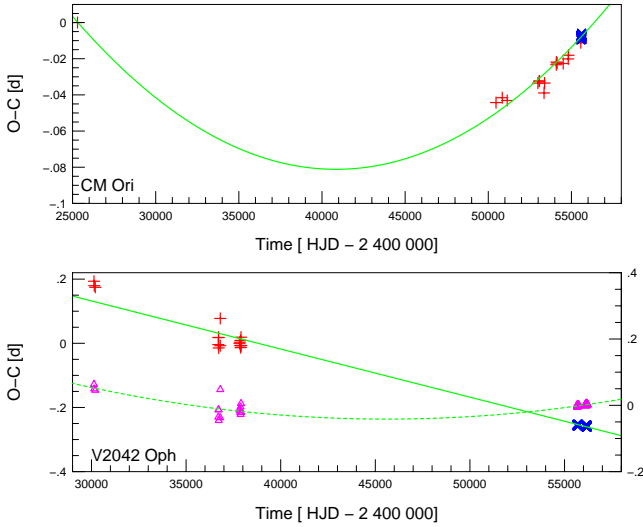
Figure 5. Long time-scale O−C diagrams of CM Ori (top) and V2042 Oph (bottom). The (red) plus symbols denote the historical data the (blue) x signs are the CoRoT measurements. The green continuous curve in the top panel shows the quadratic fit to the data. The (purple) triangles in the bottom figure mean the residual O−C data after we removed the linear trend showed by green continuous line. The right hand side vertical scale in the bottom panel belongs to the residual values, while the dashed curve shows the quadratic fit to theses data

3.2 Non-Blazhko stars

3.2.1 Stability and change of the pulsation period

As we noticed two of our stars (CM Ori and V2042 Oph) were known RR Lyrae variables. CM Ori was discovered early by Ross (1925) while V2042 Oph was found in the Sonneberg plates by Hoffmeister (1949). The stars were targets of maxima observation from time to time. The GEOS RR Lyrae data base[3] (Le Borgne et al. 2007) contains 13 and 17 maxima values for CM Ori and V2042 Oph, respectively. We completed the data set of CM Ori with three new maxima observed by TAROT Survey (Le Borgne et al. 2012) and the current CoRoT observations, while we did not use maxima of Hoffmeister (1930) because of their large uncertainties (±7 min). The constructed long-term O−C diagrams can be seen in the top panel in Fig. 5. The O−C points distribute along a parabolic function suggesting a continuous period increase. We fitted the simple quadratic formula

O − C = $at^2 + bt + c$,

where a, b, c are constants, $a = \beta$ is the linear period change rate, t is the time[4]. The rate of the period increase is $\beta = 3.37 \cdot 10^{-10} \pm 6 \cdot 10^{-12}$ dd^{-1}, or, 0.092 ± 0.002 dMy^{-1}.

The O−C diagram of V2042 Oph (bottom panel in Fig. 5) consists of the GEOS data and points from the two CoRoT runs. We shifted the 512 sec CoRoT date with

---

[4] We mention here that the GEOS data base provides Heliocentric Julian date while CoRoT uses Baricentric Julian date. The difference of these two types of dates are very tiny and therefore we neglected it.
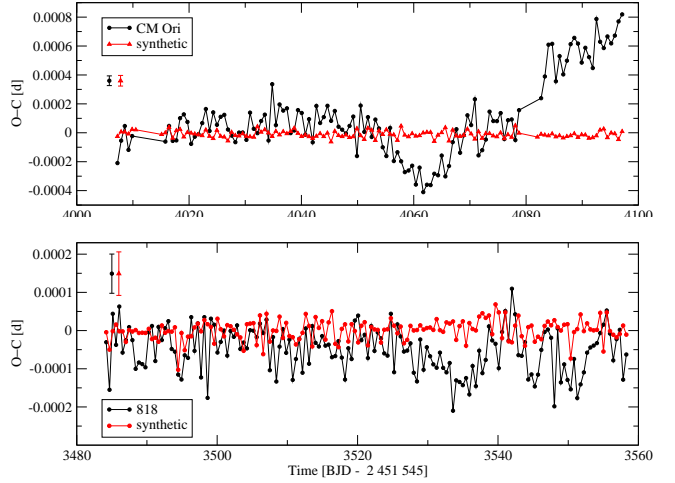
Figure 6. O−C diagrams of CM Ori (top) and #818 (bottom) constructed from the phase shifts. Black dots represent the observed data, red triangles denote the synthetic data (see the text for the details). For better visibility we show the error bars as separated symbols and we connected the consecutive points. We call the attention of the reader to the different vertical scales.

224 sec as it was described by Weingrill (2015). The O−C diagram suggests that the GEOS period (P_0=0.5385 d) is too long. From the slope of a fitted linear we get $1.5 \cdot 10^{-5}$ d correction, which is good agreement with our new CoRoT period ($P_0 = 0.53849$). Applying this correction (viz. subtracting the fitted linear shown by the continuos line) we detect a period increase again. From the quadratic fit (dashed curve) the period change rate is $\beta = 3.9 \cdot 10^{-10} \pm 2 \cdot 10^{-11}$ dd^{-1}, or, 0.11 ± 0.005 dMy^{-1}.

These period change rates are in agreement with the canonical stellar evolution models (Dorman 1992; Demarque et al. 2000; Girardi et al. 2000) which predict the red-ward evolution rate between $\alpha = 1$ and $10 \cdot 10^{-10}$ dd^{-1}, where $\alpha = \beta/P_0$. In our cases $\alpha = 5.12$, and $7.2 \cdot 10^{-10}$ dd^{-1} for CM Ori and V2042 Oph, respectively. These actual values are also fit well to the empirical rate distributions determined for the globular cluster M3 by Jurcsik et al. (2012).

After the investigation of the long term period changes we turn to the cycle-to-cycle stability of the non-Blazhko stars. Nemec et al. (2011) performed a stability analysis for the *Kepler* sample. They calculated the time dependence of the main Fourier parameters, namely $\varphi_1(t)$, $\varphi_{31}(t)$, $A_1(t)$, $R_{21}(t)$. All these functions proved to be constant with a small random scatter. Derekas et al. (2012) followed a different approach when they found random period fluctuation in the *Kepler* Cepheid V1154 Cyg. They studied the O−C diagram, which suggested the cycle lengths scatter of 0.015-0.02 d ($\approx$20-30 min), meaning $\approx 0.3\%$ of the pulsation period. Similar magnitude of cycle-to-cycle light curve fluctuation would be 1-2 minutes for a typical RR Lyrae stars. We have a chance to detect such a small time-scale effect only for the oversampled stars. Two CoRoT RRab stars CM Ori and CoRoT 103800**818** (Szabó et al. 2014) were observed in oversampled mode. Here we investigate the data sets of these two stars in details.

First we constructed the traditional O−C diagrams from the light curve maxima. Both diagrams are constant

lines with a standard deviation of $\sigma = 0.00061$ d, and 0.00132 d for CM Ori and #818, respectively. In the case of CM Ori this scatter means 0.88 min, or, 0.09% of the period, while for #818 these values are 1.9 min and 0.3%. To test the accuracy of this O−C method we prepared synthetic light curves using the Fourier solutions (amplitudes and phase) of the real stars and adding to them Gaussian noise. The noise was set that the RMS of the synthetic light curve fits became equal to the measured light curves: 0.0037 mag for CM Ori, and 0.0068 mag for #818, respectively. The standard deviation of the O−C diagrams of these stationary periodic synthetic data are $\sigma =0.00058$ d (CM Ori) and $\sigma =0.00121$ d (#818). Since we recovered the observed scatters our conclusion is that the random fluctuation of the pulsation period is lower than the detection limit of this method.

Secondly a more sensitive method was used to measure phase shifts of each pulsational cycle and transform this to an O−C diagram. This approach uses the complete light curve instead of small parts around the maxima and could result in more precise O−C values than the traditional method. The method is the same as it was successfully used by Derekas et al. (2012) for detecting the random period changes of the *Kepler* Cepheid V1154 Cyg. A template curve was defined by fitting 36th order Fourier polynomial to the phase diagram of one pulsational cycle. Then we used it – allowing only vertical and horizontal shifts – to fit each phase in the light curve. Combining the phase shifts and the period with the epoch, we calculated the O−C values which are plotted in Fig. 6 with black dots. The same process has been done for the above mentioned synthetic data as well. The results are shown in Fig. 6 with red triangles. The red and black symbols show different curve shapes for both stars. This difference is significant for CM Ori (top panel in Fig 6) but it is also less than 0.0008 d (1.2 min). What is the reason of this deviation? A frequency modulation (Blazhko effect) is unlikely because no side peaks have been detected around the harmonics in the Fourier spectrum. The rather irregular shape of these O−C curves rule out the binarity explanation. The most natural explanation is the intrinsic random period fluctuation. In other words: the RR Lyrae stars are also not precise clocks. Due to the cumulative nature of the O−C diagram we see here a random walk. A detailed discussion of the phenomenon and its appearance in O−C diagrams is given in Koen (2005).

A possible irregular period jitter in Cepheids and RR Lyrae stars was proposed by several authors (Sweigart & Renzini 1979; Deasy & Wayman 1985; Cox 1998) on different theoretical grounds. But up to now it has not been detected yet for RR Lyrae stars. It is possible that our detected small period changes of CM Ori are typical. The 1.2 min cumulative period change means no more than 1-2 seconds differences between the length of the subsequent pulsation cycles. Such a small difference could be detect only in precise uninterrapted high cadence data.

3.2.2   *Amplitude and phase behaviour of the harmonics*

The Fourier amplitude of the harmonics decreases with the harmonic order. Previously this decline was believed to be exponential but (for at least non-Blazhko stars) it was not studied. Satellite data which provide us high number of significant harmonics showed that this nearly exponentially de-

cay can not necessarily be described by a single exponential function. Both of the studied non-Blazhko RRab stars (CoRoT 101370131, Paparó et al. 2009, CoRoT 103800818 Szabó et al. 2014) show similar behaviour: their amplitudes decline exponentially for a while then this decline shows a bump then the amplitude decreases again exponentially but with a smaller exponent than with the lower order harmonics. In this section we investigate how general this feature is.

We mention here that the amplitude decline of the Blazhko stars were investigated in several papers (e.g. Smith et al. 1999; Jurcsik et al. 2005b, 2006, 2009a). These works concentrated mostly on the different declines of the harmonics and side peak amplitudes. Recently Zalian et al. (2016) found a hyperbolic fit for the harmonic decline to be better than the exponential ones. In the case of Blazhko stars, however, the amplitudes of the harmonics are heavily affected by the frequency/phase modulation part of the Blazhko effect (Benkő et al. 2011). In other words, in the amplitude decline behaviour the basic physics of the pulsation and unknown aspects of the Blazhko effect are mixed. To avoid this complication we restricted our study to the non-Blazhko stars.

Our sample contains six non-Blazhko RR Lyrae stars. We completed this sample with the three formerly discussed non-blended CoRoT stars (CoRoT 101370**131**, CoRoT 103800**818**, CoRoT 104315**804**, Szabó et al. 2014). The used Fourier parameters A_i and φ_i of these stars are given in an electonic-only table[5].

If we plot the Fourier amplitude ratios $R_{n1} = (A_n/A_1)$ as a function of the harmonics n for these nine CoRoT non-Blazhko stars we get Fig. 7. In this logarithmic plot we see that the monotonic decay holds to the 5-15th harmonic order. The exact value varies from star to star. The distribution curves seem to build up a sequence from the stars #804, where only a slight break appears at the 5th harmonic, to the star #818, where a deep minimum exists at around the 15th harmonic. It can also be realized that the depth of the dip tends to increase with the increasing harmonic order. This trend seems to break at #739, but its dip is defined by only one small (marginally significant) amplitude of the 12th harmonic frequency, the extraordinarily deep minimum might cause this uncertainty. The order of stars settled by the diagram in Fig. 7 is almost the same as the order of decreasing pulsation period. The longest period non-Blazhko star of the sample is #804 ($P_0 = 0.7218221$ d), while the shortest one is the star #818 ($P_0 = 0.4659348$ d). Seven stars from the nine one follow this period length order. The two exceptions are #902 and #259 which are located in longer period positions of the sequence than their real period.

The Fourier amplitudes and phases collectively contain the complete information of a signal. Although this is well-known, the phase spectra are studied much less frequently than the amplitude ones. In the right-hand-side panel of Fig. 7 we show the epoch independent phase differences φ_{n1} of the nine studied RRab stars. The panel shows the phase differences according to the definition: $\varphi_{n1} = \varphi_n - n\varphi_1$ (n

---

[5] The table contains all stars' data consecutively. In the three columns are the frequency in d^{-1}, the amplitude in CoRoT magnitude, and the phase in radian.
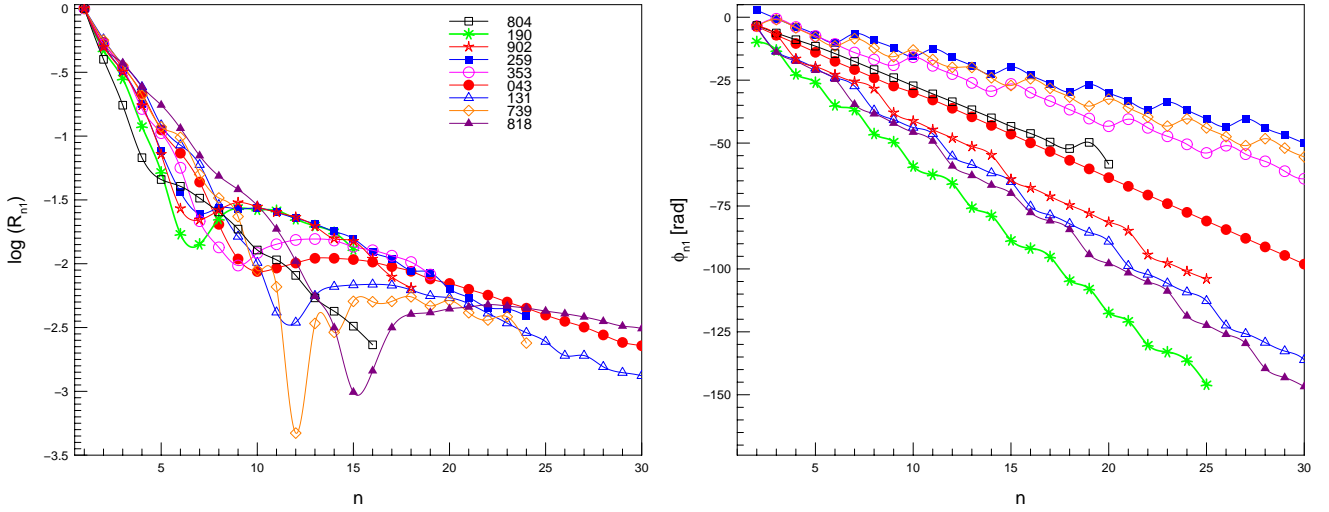
Figure 7. Left panel Amplitude ratio R_{n1} distribution of the non-Blazhko stars vs. harmonic order n. Each symbol represents an amplitude ratio of a given star. The amplitude ratios belonging to a different star denoted by different symbols (see the legend in the top right corner of the figure). The consecutive amplitude ratios of a given star are connected with a continuous line for the better visibility. Right panel Epoch independent phase differences φ_{n1} vs. harmonic orders n. As opposed to the common handling the phase differences are not transformed to a restricted interval (e.g. $0 < \varphi_{n1} < 2\pi$), for the sake of the better visibility.
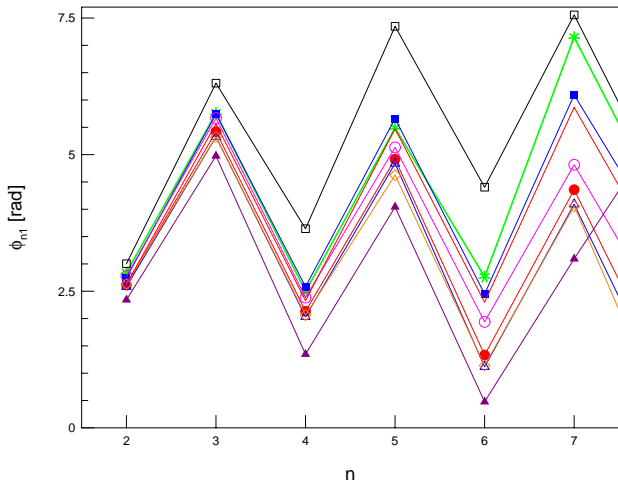

Figure 8. The low order phase differences plotted on the usual scale. The designations are the same as in the right hand side panel of Fig. 7.

integer), where we did not transform the differences to a restricted interval as it is common. The reason is illustrated with the Fig. 8 where we transformed the first seven φ_{n1} quantities into the $(0, 5/2\pi)$ interval. Here the $\varphi_{n1}(n)$ distributions of different stars are mixed. The distributions are hardly traceable.

By looking at the right panel in Fig. 7 we notice that these $\varphi_{n1}(n)$ distribution functions are deviate from each other. The distance of the nearby functions increases with the increasing harmonic order forming a fan shape structure on the $\varphi_{n1}(n) - n$ surface. This spread suggests that the fine structure of the individual stars' light curve differ more than their main character described with the low order harmonics.

The shape of these $\varphi_{n1}(n)$ decline functions vary form the middle of the fan-shape distribution to the wings: from the pure linear (#043) to intensely crisscross shapes (e.g. #259, #190), respectively.

The fine structures of the light curves such as the amplitude distribution of the higher harmonics have never been studied theoretically. Stellingwerf & Donohoe (1987) estimated Fourier parameters R_{n1} and φ_{n1} for $n \leq 10$ using a simple non-adiabatic one-zone pulsation model. They did not investigate the amplitude ratio and phase difference distributions with respect to the harmonic orders, but their figures fig. 6-7. suggest monotonic declining amplitudes with the increasing n, except some model light curves, where their 'acuteness' parameter is small. In these cases the higher order amplitudes ($n \geq 7$) could be higher than the lower ones. The phase plots in their fig. 8-9. predict monotonic increasing phase differences (within the interval $0 \leq \varphi_{n1} \leq 3\pi$) at least until $n \leq 6$, which is evidently not the case for the observed light curves (see Fig. 8). The amplitude ratios and phase differences of theoretical light curves were investigated by Dorfi & Feuchtinger (1999) using a more enhanced non-linear convective 1D pulsation approach but their calculations extended up to the 5th harmonic order only. The more realistic physical treatment gives more realistic predictions for phase differences (see fig. 8 in the paper)[6]. Reading the related values from the different panels we can recognize a similar crisscross behaviour of the phase difference distribution as we see in our Fig 8.

We compared the Fourier amplitude and phase distribution of the observed and model light curves calculated from the photospheric temperature $T(t)$ and gravitational acceleration $\log g(t)$ curves by the Florida-Budapest

---

[6] The phases used for that plot coming from a cosine decomposition. They need to shift (e.g. $\varphi_{21} = \Phi_{21} - \pi/2$, $\varphi_{31} = \Phi_{31} + \pi$) for a direct comparison to our work.
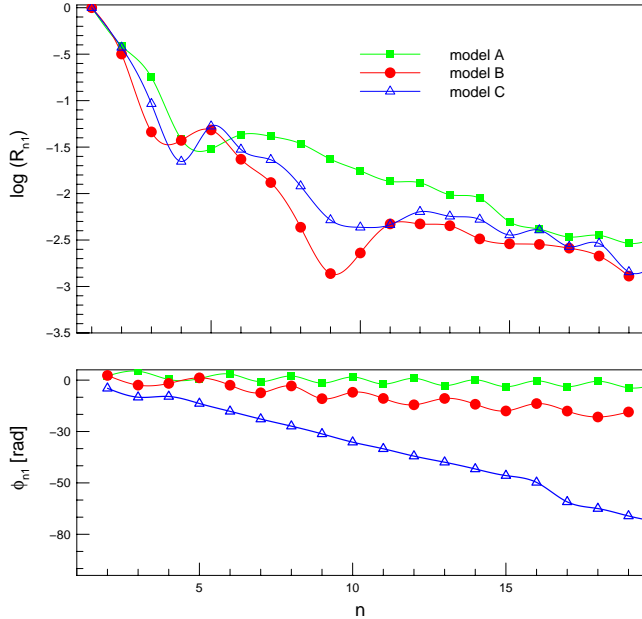
Figure 9. Amplitude ratio distribution $R_{n1}(n)$ (top panel) and epoch independent phase differences φ_{n1} vs. harmonic orders n (bottom panel) of some synthetic light curves.

hydrocode (Kolláth & Buchler 2001; Kolláth et al. 2002). Since the models use the exact black-body condition we can use these photospheric quantities instead of the effective ones. We investigated three different model light curves denoted by A, B and C. The input parameters of the model A are: $M = 0.65$ M$_\odot$ (stellar mass), $L =40$ L$_\odot$ (luminosity), $T_{\rm eff} = 6477$ K (the effective temperature of the input static model), Z=0.0001 (metal content). For model B these parameters are: $M = 0.77$ M$_\odot$, $L =50$ L$_\odot$, $T_{\rm eff} = 6300$ K, Z=0.004; and model C: $M = 0.71$ M$_\odot$, $L =40$ L$_\odot$, $T_{\rm eff} = 6300$ K, Z=0.004.

For the direct comparison we have to prepare synthetic CoRoT light curves from the model outputs: $T_{\rm eff}(t)$, $\log g(t)$. Using the basic formula of synthetic photometry (Bessell 2005) we determine the detected stellar fluxes in photon numbers $N_{\rm p}$ as

$$N_{\rm p} = \frac{1}{hc} \int F(\lambda)\lambda R(\lambda)S(\lambda)d\lambda, \qquad (1)$$

where $F(\lambda)$ is the spectrum of a star in energy units, $R(\lambda)$ is the response function of the system, $S(\lambda)$ is the filter function, λ is the wavelength, h is the Planck constant and c is the speed of light. The flux was computed by using the CoRoT equipment's spectral response function $R(\lambda)$ given by Auvergne et al. (2009) and without filter function ($S(\lambda) = 1$). Let us denote the result of this computation by $N_{\rm p}^{\rm C}$, and the artificial CoRoT magnitude is $m_{\rm CoRoT} = -2.5\log(N_{\rm p}^{\rm C}) + c$, where c is an arbitrary constant. We used the enhanced Kurucz models (Castelli et al. 1997) provided by the Spanish Virtual Observatory[7] as theoretical flux distribution functions $F(\lambda)$. A set of model spectra (360 synthetic spectra) were chosen which cover the

physical parameters ($T_{\rm eff}$, $\log g$) of different pulsation phases and the metallicity range of the RR Lyrae stars, namely, $T_{\rm eff}$ is between 5750 and 8000 K, $\log g$ 2.5 and 5.0, while [Fe/H] is between 0 and -2.5 dex. Although these static model atmospheres are not optimal for all RR Lyrae pulsation phases (see eg. Barcza 2010; Barcza & Benkő 2014) without available, adequate dynamical model atmospheres we can use them as a first approximation. By using $T_{\rm eff}(t)$ and $\log g(t)$ functions from the pulsation model we assigned an interpolated $m_{\rm CoRoT}$ value to each pulsation phase. Generating the artificial CoRoT light curves by this way corresponds to a phase dependent bolometric correction which was done by Kovács & Kanbur (1998) for V band.

The Fourier solutions of the synthetic light curves are presented in Fig. 9 in the same form as the observed ones in Fig. 7. The amplitude distribution of model A in top panel show similar decline to the observed curves, however, the higher metallicity models B and C show double bumps. We have not seen such behaviour for any of the real stars. It is not clear, which one of the two dips correspond to the observed single dip. The phase difference distributions in bottom panel of Fig 9 are phenomenological similar to the observed data (left panel in Fig. 7), but the numerical φ_{n1} values of model A are unusually high. We conclude that recent 1D hydrodynamic models can not reproduce the fine structure of the observed light curves of the RR Lyrae stars even in the simplest non-modulated fundamental mode pulsating case. Maybe the enhanced versions of the first successful multidimensional computations (2D/3D Mundprecht et al. 2013; Geroux & Deupree 2015) will provide us better synthetic light curves. For a perfect agreement between observation and theory we probably have to wait for sophisticated dynamical atmosphere models as well. We call the readers' attention to the diagrams in Fig. 7, which presents a potentially sensitive tool for quantitative study of the fine structures of RR Lyrae light curves.

4 ESTIMATION FOR PHYSICAL PARAMETERS

The standard photometric V light curves of RR Lyrae stars allow us to estimate their physical parameters such as metallicity, effective temperature, $\log g$, mass, etc. by using empirical formulae (e.g. Jurcsik & Kovács 1996; Jurcsik 1998; Kovács & Walker 2001). However, neither chromatic nor monochromatic CoRoT light curves are calibrated to standard photometric systems. In principle, this calibration is possible, but no one has published such attempts yet. The basic idea of such a transformation along with some of its inherent problems is discussed in Weingrill (2015). Similar transformation problems were successfully solved by Nemec et al. (2011) who had to deal with light curves in *Kepler* $K_{\rm p}$ band. They compared the *Kepler* light curves with the existing Johnson V light curves of three non-modulated RRab stars, then they determined numerical shifts for all useful Fourier parameters. Using these transformed parameters and formulae for the V filter they received noticeably good estimates for the physical parameters which were then verified by high-resolution spectroscopy (Nemec et al. 2013). A different approach was developed by the OGLE team. Since the OGLE-III RR Lyrae data (Soszyński et al. 2009)
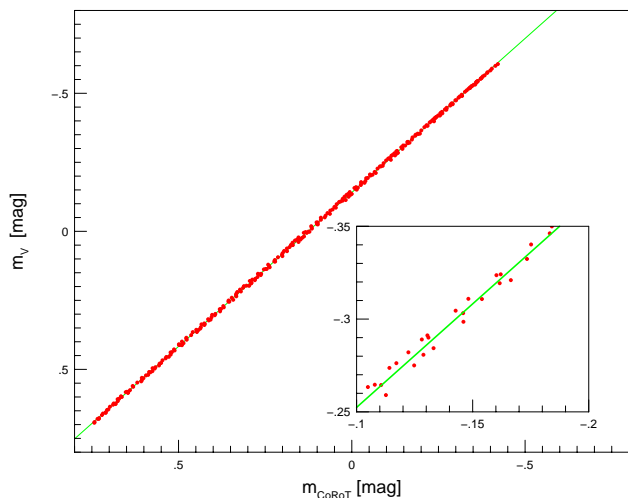
Figure 10. Correlation between the synthetic monochromatic CoRoT (m_{CoRoT}) and synthetic Johnson V (m_V) magnitudes. The insert shows a zoom from the plot demonstrating the weak dependence of the relation on secondary parameters (metallicity, $\log g$).

are predominantly observed in Cousins I colour, empirical formulae for I filter data were needed for physical parameter estimation. The OGLE team independently calibrated the empirical relations (Smolec 2005; Pietrukowicz et al. 2012) instead of transforming the existing formulae relevant for the V passband.

4.1 Colour transformation of the CoRoT data

A complete calibration of CoRoT coloured and monochromatic data is out of the scope of this paper. Instead of this we use two alternate transformations achieving the necessary data. Our primary goal is to check the physical parameters of our sample and to select special stars – if there are any – for further investigation. For this purpose a rough physical parameter estimation is enough which can be available through these approximate transformations.

(1) Due to the direct analogy of CoRoT monochromatic and *Kepler* unfiltered K_{p} data we applied the method used by Nemec et al. (2011). Unfortunately, standard V observations of CoRoT RR Lyrae stars are even more sparse than Kepler stars' measurements. We found one (almost) complete phase curve for CoRoT 101370131 in Szabó et al. (2014). Fourier parameters were obtained from SuperWASP data by Skarka (2015) for CM Ori. From these two data sets we derived the two most important Fourier parameters:

$$A_1^V = A_1^{\mathrm{CoRoT}} + (0.10 \pm 0.04),$$
$$\varphi_{31}^V = \varphi_{31}^{\mathrm{CoRoT}} - (0.05 \pm 0.04),$$

where A_1 denotes the Fourier amplitude of the main pulsation frequency, φ_{31} epoch independent phase difference is defined in the usual way: $\varphi_{31} = \varphi_3 - 3\varphi_1$ (Simon & Lee 1981), where φ_1 and φ_3 are the Fourier phases of the main frequency and the second harmonic. The upper indices denote the used filter system.

(2) Because of the evident weaknesses of the previous

transformation we alternatively applied the synthetic photometry approach (eg. Straižys 1996; Bessell 2005). This method allow us to transform the CoRoT monochromatic RR Lyrae observations to the standard Johnson V light curves to which we can apply the empirical relations directly. Following the basic idea of synthetic photometry (Bessell 2005) we determine the detected stellar fluxes in photon numbers N_{p} as it was shown in Eq. 1. In our case, the flux was computed twice, once by using the CoRoT equipment's spectral response function $R(\lambda)$ given by Auvergne et al. (2009) and second without the filter function. Let us denote the result of this computation by N_{p}^C. Second, by using the same $R(\lambda)$ function combined with the Bessell V filter function $S(\lambda)$ (Bessell 1990) we get N_{p}^V. We utilized the same set of model spectra (360 synthetic spectra) was used for the computation of synthetic CoRoT light curves in Sec. 3.2.2.

We correlated the synthetic CoRoT magnitudes $m_{\mathrm{CoRoT}} = -2.5 \log_{10} N_{\mathrm{p}}^C + c_1$ to the synthetic V magnitudes: $m_V = -2.5 \log_{10} N_{\mathrm{p}}^V + c_2$. The average of all our light curves transformed to the magnitude scale are set to zero, that defines a kind of 'relative' magnitude. By using these light curves we avoid the need to determine the absolute zero point of the synthetic photometry which is generally a difficult problem. Here we can set the constants c_1 and c_2 arbitrarily. We have chosen these so that the resulted magnitude ranges are similar to the observed amplitudes of RRab stars and the zero point of the fitted line is zero. The correlation between the synthetic CoRoT and the V magnitudes is shown in Fig. 10. The best-fitted linear relation is

$$m_V = 1.1157(\pm 0.0008) m_{\mathrm{CoRoT}}. \tag{2}$$

The insert in Fig. 10 demonstrates the dependence of the relation on physical parameters such as metallicity, or $\log g$. This virtual 'scatter' is an intrinsic physical property of the stars and not a scatter due to the uncertainty of our method. Using the ratio in Eq. 2 we derived the transformed V light curves, from which we deduced the Fourier parameters (amplitudes and phase differences) necessary to use the empirical formalae.

4.2 Physical parameters

Since no physical parameters have been derived for any of the CoRoT RR Lyrae stars, yet, we estimated the basic physical parameters of the complete CoRoT RRab sample. Only three blended stars (CoRoT 101315488, 100881648, and 101503544) were omitted, because of their small amplitude distorted light curves (see Szabó et al. 2014) resulted in unusable Fourier parameters. Although the empirical formulae were originally calibrated on the non-Blazhko stars, since then some works showed that the formulae can be applied for well-sampled Blazhko stars as well (Kovács 2005; Smolec 2005; Jurcsik et al. 2009b, 2012; Nemec et al. 2013; Skarka 2015).

The calculations were done for the above (1) and (2) transformed data sets, independently. The metallicity was determined by using the Jurcsik & Kovács (1996) formula, which is defined on the Carretta & Gratton (1997) scale. These metallicity values can be transformed to the Zinn & West (1984) scale as it was showed by Sandage (2004). There are signs that the formula of Jurcsik & Kovács (1996) gives systematically higher metallicity in the case

Table 2. Estimated physical parameters of the CoRoT RRab stars. The columns contain the CoRoT ID, the estimated physical parameters obtained form empirical formulae: the metallicity [Fe/H], the absolute visual brightness M_V, the reddening-free colour index $(B-V)_0$, the surface gravitational acceleration $\log g$, the effective temperature T_{eff}, and the mass M. Last column contains remarks on the Blazhko nature, or (for star #793) the date of the observing runs. The upper indices (1) and (2) denote the two used colour transformation methods (see the text for the details). The comma separated values show the results obtained from the transformed data of method (1) and (2), respectively.

Corot ID	[Fe/H]$^{(1),(2)}$	$M_V^{(1),(2)}$ [mag]	$(B-V)_0^{(1),(2)}$ [mag]	$\log g$	$T_{\text{eff}}^{(1),(2)}$ [K]	$\log L^{(1),(2)}$	$M^{(1),(2)}$ [M$_\odot$]	rem.
100689**962**	$-0.75,-0.65$	0.867,0.900	0.314,0.324	3.023	6730,6694	1.519,1.524	0.71,0.75	Bl, $D_{\text{m}} > 3$
101128**793**	$-0.75,-0.64$	0.737,0.767	0.326,0.335	2.872	6632,6600	1.546,1.534	0.52,0.52	Bl, $D_{\text{m}} > 3$
101370**131**	$-1.32,-1.22$	0.539,0.568	0.347,0.355	2.728	6436,6407	1.674,1.663	0.57,0.57	$D_{\text{m}} > 3$
102326**020**	$-0.66,-0.56$	0.501,0.538	0.395,0.407	2.612	6248,6207	1.687,1.667	0.52,0.51	Bl, $D_{\text{m}} > 3$
103800**818**	$-0.97,-0.86$	0.675,0.699	0.305,0.312	2.879	6714,6694	1.578,1.564	0.54,0.53	
103922**434**	$-1.22,-1.11$	0.612,0.641	0.330,0.338	2.799	6547,6520	1.627,1.612	0.56,0.55	Bl
104315**804**	$-0.55,-0.45$	0.557,0.594	0.387,0.399	2.646	6304,6263	1.661,1.641	0.51,0.50	$D_{\text{m}} > 3$
104948**132**	$-0.97,-0.87$	0.605,0.635	0.344,0.353	2.757	6492,6461	1.635,1.619	0.54,0.53	Bl
105288**363**	$-1.13,-1.02$	0.643,0.677	0.354,0.364	2.775	6435,6398	1.613,1.595	0.55,0.54	Bl
205924**190**	$-1.28,-1.18$	0.514,0.552	0.392,0.403	2.648	6210,6167	1.682,1.667	0.56,0.56	
605307**902**	$-1.03,-0.92$	0.605,0.640	0.367,0.377	2.724	6372,6333	1.636,1.623	0.54,0.54	
617282**043**	$-1.39,-1.28$	0.484,0.512	0.348,0.355	2.697	6418,6393	1.700,1.685	0.57,0.56	
651349**561**	$-0.26,-0.15$	0.702,0.740	0.375,0.387	2.735	6415,6371	1.588,1.567	0.49,0.48	Bl, $D_{\text{m}} > 3$
655183**353**	$-1.26,-1.16$	0.500,0.534	0.371,0.381	2.667	6312,6278	1.691,1.663	0.56,0.53	
657944**259**	$-0.54,-0.43$	0.673,0.706	0.353,0.363	2.765	6497,6461	1.601,1.582	0.51,0.50	
659723**739**	$-0.89,-0.78$	0.642,0.670	0.330,0.338	2.803	6581,6553	1.608,1.598	0.53,0.53	2011, $D_{\text{m}} > 3$
659723**739**	$-0.94,-0.84$	0.656,0.687	0.337,0.346	2.803	6540,6508	1.604,1.588	0.54,0.53	2012, $D_{\text{m}} > 3$

of very low metallic content (see. e.g. Jurcsik & Kovács 1996; Nemec 2004; Nemec et al. 2013), although for example Skarka (2015) found no strong evidence suggesting this. Since our sample does not contain lower metallicity stars than [Fe/H] $\lesssim -1.3$ dex, we prefer the Carretta-Gratton metallicity scale as the best-fit one to the high resolution spectroscopy. The extinction free colour index $(B-V)_0$ and $\log g$ were calculated from the formulae of Jurcsik (1998), while for the absolute magnitude determination we followed Nemec et al. (2013), Lee et al. (2014), and Skarka (2015) who applied a 0.2 zero point shift to the formula of Jurcsik (1998). The effective temperature was estimated by the formula of Kovács & Walker (2001).

The empirical formulae for the two fundamental parameters: the stellar mass and luminosity are yielded systematically different results depending on whether they come from the pulsation (Jurcsik 1998) or the stellar evolution (Sandage 2006; Bono et al. 2007) models. These discrepancies were discussed in the case of *Kepler* RRab sample by Nemec et al. (2011) in details. More recently, however, Marconi et al. (2015) constructed consistent pulsation models where the stellar masses and luminosities were fixed according to the horizontal-branch evolutionary models. We took into account these new results when we computed the masses and luminosities from the Jurcsik (1998) formulae than we fixed either of these parameters and determine the other one by the van Albada-Baker type relation given by Marconi et al. (2015) (eq. 1 in the paper). The typical result of this cross check is that the pulsation mass defined by Jurcsik (1998) formula needs higher luminosity for consistency than that we get from the Jurcsik (1998) luminosity formula. Or vice verse: Marconi et al. (2015) relation yields lower mass if we use Jurcsik (1998) luminosities. But in the latter case the calculated small masses are out of the al-

lowed parameter range where the stable pulsation persists. Therefore, we kept the pulsation masses and determined the luminosities by the Marconi et al. (2015) formulae. We mention here that for two stars (#793 and #363) the alternate calculations provided consistent values for both masses and luminosities, and for #962 the pulsation mass (0.52 M$_\odot$) resulted in such low luminosity ($\log L$=1.416 dex) which is below the horizontal branch for the given metallicity. We accept the evolutionary mass and pulsation luminosity for #962.

The results are summarized in Table 2. In spite of the rather ad hoc character of the two colour transformations the estimated parameters are surprisingly consistent. The differences between the comma separated columns (obtained from the two transformations) indicate the accuracy of the estimated parameters. We checked the consistency of the light curve shapes with the calibration sample of the empirical formulae using the D_{m} parameter (Jurcsik & Kovács 1996). Several Blazhko stars yield $D_{\text{m}}<3$ values which supports that their estimated physical parameters should be as good as the non-Blazhko stars' ones. There is a rather surprising result of this test: for three non-Blazhko stars (#131, #804, and #739) $D_{\text{m}}>3$ which suggests some light curve distortion. We compared the observed individual Fourier parameters of these stars with the calculated ones by the interrelation of Jurcsik & Kovács (1996). We found that the observed amplitudes (e.g. A_1) are always smaller that the predicted ones. This implies some flux loss for these stars. This would not be unprecedented. Similar problems have been discussed for several *Kepler* RR Lyrae stars (Benkő et al. 2014). The explanation of the possible flux lost is simple: the star fluxes are collected within pre-defined pixel masks for both CoRoT and *Kepler*. In the preparatory phase of the missions photometric sky surveys had been conducted
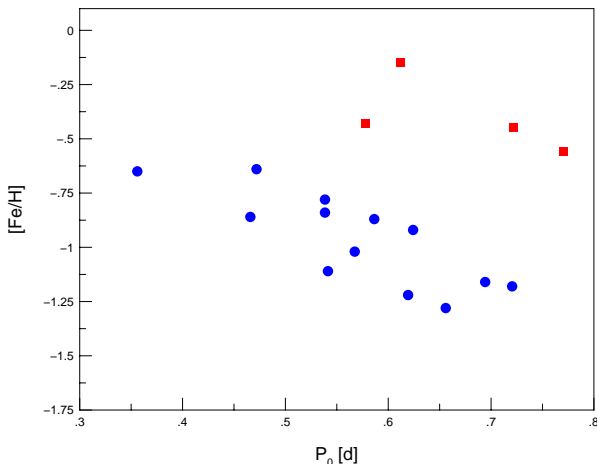
Figure 11. Correlation between the pulsation period P_0 and the metallicity [Fe/H][(2)]. The blue dots define a moderate metalliciy stellar group with the average metalliciy of $<$[Fe/H]$>$=-0.96 dex, while red squares show a higher metallic content group with $<$[Fe/H]$>$=-0.39 dex. The red square between the two groups shows the star #259 with $<$[Fe/H]$>$=-0.43 dex.

and the brightness values of the input catalogues (Exo-DAT, KIC) define the size of the masks. Since these missions are optimized to detect small brightness variations (transiting exoplanets, solar type oscillations) this strategy is generally appropriate. However, the RR Lyrae stars have large amplitudes with highly non-sinusoidal light curve shapes, viz. they spend most of their time in faint phases. If a mask is fitted to this faint state, it is too small around maximal brightness resulting in flux loss. This hypothesis is strengthened by the fact that these problematic stars (#131, #804, and #739) are the faintest (15.6, 15.94, and 15.186 mag) non-Blazhko RR Lyrae stars in the Exo-DAT catalogue. Additionally, the star #739 was observed using different masks for the two runs (LRc07 and LRc10). The light curves of the two runs are different, e.g. they show different amplitudes and other Fourier parameters are also slightly different. If both masks contained the total flux no such differences would be expected.

The original goal of this parameter estimation was to find any extreme stars in our sample. The physical parameters of all stars are, however, in the canonical ranges of the equilibrium values of RRab stars. The metallicity is between $-0.15 >$ [Fe/H] > -1.39, the absolute visual brightness is $0.9 > M_V > 0.484$ mag, the reddening free color index is $0.305 > (B - V)_0 > 0.407$, the effective temperature is $6210 > T_{\rm eff} > 6730$ K, the surface gravitational acceleration is $3.023 > \log g > 2.612$, the luminosity is $1.700 > \log L > 1.519$, and the mass is $0.75 > M > 0.48$ M$_\odot$. By reviewing some classical diagnostic diagrams of RR Lyrae stars such as period vs. amplitude, $(B - V)_0$ vs. M_V, etc. we found that the CoRoT sample consists of two distinct groups. The separation of the two groups is the best seen in period vs. metallicity diagram (see Fig. 11). The blue symbols of the figure define a moderately metal poor group with an average metallicity of $<$[Fe/H]$>=-0.96$ dex, while the red filled squares denote the most metal rich stars of the sample (#020, #804, #561, $<$[Fe/H]$>=-0.39$ dex) and

the star #259 which is located at an intermediate position between of these two groups. The metal rich group has significantly higher average period $<P_0>$=0.7013 d than the more populous metal poorer group $<P_0>$=0.5677 d. These stars are at the red edge when we plot the sample in the theoretical HR diagram ($\log T_{\rm eff}$, $\log L$). This is not a surprise, since the instability strip moves red-ward with the increasing metallicity.

5 SUMMARY

We presented here the results of a rigorous RR Lyrae search in the CoRoT archive. We found nine RRab stars in the data base that have not been studied and seven of them are new discoveries.

Three stars show the Blazhko effect. The cycle-to-cycle variation of these Blazhko effects are evident either for amplitude or frequency modulations or both which rises the possibility of their multiperiodic (or irregular/chaotic) nature. The Fourier spectrum of star #132 contains small amplitude 'additional' frequencies which can be identified as the consequence of the period doubling effect and the excitation of the second radial overtone mode. The later mode identification is strengthened by pulsation modeling, since the observed period ratio is unusually high ($P_2/P_0 = 0.601$), but linear pulsation models at least do not exclude this period ratio. The other two Blazhko stars show no significant additional frequencies.

The light curve stability and period changes were studied for non-Blazhko stars. We detected a significant cycle-to-cycle fluctuation of the pulsation period (cycle length) of CM Ori. This is the first case that random jitter has been detected for an RR Lyrae star. The fluctuation rate is tiny: at longest 1-2 seconds per cycles.

Long term period changes were also investigated for the two known RR Lyrae stars CM Ori and V2042 Oph. Their O$-$C diagrams cover more than 80 and almost 70 years, respectively. Both stars show a slight period increase with rates which agree well with the prediction of the stellar evolution theory for normal red-ward evolution.

The Fourier amplitude and phase difference distribution with respect to the harmonic order have been studied for the first time on a larger set of non-Blazhko stars. We found a common amplitude decline feature. The phase differences show a split distribution. The observed distributions were compared theoretical works. Our conclusion is that the recent model calculations reproduce the main features but the fine structures can not be described properly. These amplitude and phase distribution diagrams could be potential diagnostic tools for constraining pulsation models, because of their high sensitivity of the fine structure of the light curves.

We successfully transformed the CoRoT unfiltered light curves, and their Fourier parameters to the Johnson V curves, and parameters. As a by-product of the use of the interrelations we found possible flux loss for several stars. Such an effect was shown for high amplitude variables of the *Kepler* telescope, but has not documented yet in the case of CoRoT satellite.

By using empirical formulae we estimated the basic physical parameters of the complete CoRoT RRab sample.

The estimated physical parameters define two subgroups of the sample. (1) A shorter period and lower metallicity and (2) a longer period higher metallicity groups. The physical parameters of both groups, however, are within the canonical ranges of RR Lyrae stars.

ACKNOWLEDGEMENTS

REFERENCES

Auvergne, M., Bodin, P., Boisnard, L. et al. 2009, A&A, 506, 411
Baglin, A. Auvergne, M., Boisnard, L. et al. 2006, in 36th COSPAR Scientific Assembly, ed. A. Wilson, ESA SP 1296, (ESA, Noordwijk), 3749
Barcza, S. 2010, MNRAS, 406, 486
Barcza, S. & Benkő, J.M. 2014, MNRAS, 442, 1863
Benkő, J. M. & Szabó, R. 2015, ApJ, 809, L19
Benkő, J. M., Kolenberg, K., Szabó, R. et al. 2010, MNRAS, 409, 1585
Benkő, J. M., Szabó, R., & Paparó, M. 2011, MNRAS, 417, 974
Benkő, J. M., Palchy, E., Szabó, R., Molnár, L., & Kolláth, Z. 2014, ApJS, 213, 31
Bessell, M. S. 1990, PASP, 102, 1181
Bessell, M. S. 2005, ARA&A, 43, 293
Bono, G., Caputo, F., & Di Criscienzo, M. 2007, A&A, 476, 779
Borucki, W. J. et al. 2010, Science, 327, 977
Carretta, E. & Gratton, R. G. 1997, A&AS, 121, 95
Castelli, F, Gratton, R. G., & Kurucz, R. L. 1997, A&A, 318, 841
Chadid, M. 2012, A&A, 540, A68
Chadid, M., Benkő, J. M., Szabó, R. et al. 2010, A&A, 510, A39
Cox, A. N. 1998, ApJ, 496, 246
Deasy, H. P. & Wayman, P. S. 1985, MNRAS, 212, 395
Debosscher, J. Sarro, L. M., López, M. et al. 2009, A&A, 506, 519
Deleuil, M., Meunier, J. C., Moutou, C. et al. 2009, AJ, 138, 649
Demarque, P., Zinn, R., Lee, Y.-W. & Yi, S. 2000, AJ, 119, 1398
Derekas, A., Szabó, Gy. M., Berdnikov, L., et al, 2012, MNRAS, 425, 1312
Dorfi, E. A. & Feuchtinger, M. U. 1999, A&A, 348, 815
Dorman, B. 1992, ApJS, 81, 221
Geroux, C. M., & Deupree, R. G. 2015, ApJ, 800, id.35
Girardi, L., Bressan, A., Bertelli, G. & Chiosi, C. 2000, A&AS, 141, 371
Hoffmeister, C. 1930, Astron. Nachr., 238, 17
Hoffmeister, C. 1949, Astron. Abh. Ergänzungshefte z.d. Astron. Nachr., 12, No 1, A3
Jurcsik, J. 1998, A&A, 333, 571
Jurcsik, J. & Kovács, G. 1996, A&A, 312, 111
Jurcsik, J., Szeidl, B., Nagy, A., & Sódor, Á. 2005a, Acta Astron., 55, 303
Jurcsik, J., Sódor, Á., Váradi, M., et al. 2005b, A&A, 430, 1049
Jurcsik, J., Szeidl, B., Sódor, Á., et al. 2006, AJ, 132, 61
Jurcsik, J., Hurta, Zs., Sódor, Á., et al. 2009a, MNRAS, 397, 350
Jurcsik, J., Sódor, Á., Szeidl, B. et al. 2009b, MNRAS, 400, 1006
Jurcsik, J., Hajdu, G., Szeidl, B. et al. 2012, MNRAS, 419, 2173
Koen, C. 2005, in The Light-Time Effect in Astrophysics, ed. C. Sterken, ASP Conf. Ser. 335, (ASP, San Francisco), 25
Kolenberg, K., Szabó, R., Kurtz, D. W. et al. 2010, ApJ, 713, L198
Kolláth, Z. 1990, Konkoly Observatory Occasional Technical Notes, No. 1, 1
Kolláth, Z., & Buchler, J. R. 2001, in Stellar Pulsation âĂŞ Non-linear Studies, eds. Takeuti, M. & Sasselov, D. D., ASS Library Series vol. 257, (Kluwer Academic Publishers, Dordrecht), 29
Kolláth, Z., Buchler, J. R., Szabó, R., & Csubry, Z. 2002, A&A, 385, 932
Kolláth, Z., Molnár, L., & Szabó, R. 2011, MNRAS, 414, 1111
Kovács, G. 2005, A&A, 438, 227
Kovács, G. & Kanbur, S. 1998, MNRAS, 295, 834
Kovács, G. & Walker, A. R. 2001, A&A, 371, 579
Le Borgne, J.-F., Paschke, A., Vandenbroere, J. et al. 2007, A&A, 476, 307
Le Borgne, J.-F., Klotz, A., Poretti, E. et al. 2012, AJ, 144, 39
Lee, J.-W. López-Morales, M., Hong, K. al. 2014, ApJS, 210, 6
Marconi, M., Coppola, G., Bono, G., et al. 2015, ApJ, 808, 50
Molnár, L., Szabó, R., Moskalik, P. et al. 2015, MNRAS, 452, 4283
Moskalik, P., Smolec, R., Kolenberg, K. et al. 2015, MNRAS, 447, 2348
Mundprecht, E., Muthsam, H. J., & Kupka, F. 2013, MNRAS, 435, 3191
Nemec, J. M. 2004, AJ, 127, 2185
Nemec, J. M., Smolec, R., Benkő, J. M. et al. 2011, MNRAS, 417, 1022
Nemec, J. M., Cohen, J. G., Ripepi, V. et al. 2013, ApJ, 773, 181
Paparó, M., Szabó, R., Benkő, J. M. et al. 2009, in Stellar Pulsation: Challanges for Theory and Observation, AIP Conf. Ser. Vol. 1170., ed. J. A. Guzik & P. A. Bradley, 240
Pietrukowicz, P., Udalski, A., Soszyński, I. et al. 2012, ApJ, 750, 169
Poretti, E. Paparó, M., Deleuil, M. et al. 2010, A&A, 520, A108
Ross, F. E. 1925, AJ, 36, 99
Sandage, A. 2004, AJ, 128, 858
Sandage, A. 2006, AJ, 131, 1750
Simon, N. R. & Lee, A. S. 1981, ApJ, 248, 291
Skarka, M. 2015, MNRAS, 445, 1584
Smith, H. A., Barnett, M., Silbermann, N. A., & Gay, P. 1999, AJ, 118, 572
Smolec, R. 2005, Acta Astron., 55, 59
Soszyński, I. Udalski, A., Szymański, M. K. et al. 2009, Acta Astron., 59, 1
Soszyński, I. Udalski, A., Szymański, M. K. et al. 2014, Acta Astron., 64, 177
Stellingwerf, R. F. & Donohoe, M. 1987, ApJ, 314, 252
Sterken, C. 2005, in The Light-Time Effect in Astrophysics, ed. C. Sterken, ASP Conf. Ser. 335, (ASP, San Francisco), 3
Straižys, V. 1996, Baltic Astron., 5, 459
Sweigart, A.V. & Renzini, A. 1979, A&A, 71, 66
Szabó, R., Kolláth, Z., Molnár, L. et al. 2010, MNRAS, 409, 1244
Szabó, R., Benkő, J. M., Paparó, M. et al. 2014, A&A, 570, A100
Weingrill, J. 2015, Astron. Nachr., 336, 125
Zalian, C., Chadid, M., Vernin, J., et al. 2016, MNRAS, 456, 192
Zinn, R. & West, M. J. 1984, ApJS, 55, 45

This paper has been typeset from a TEX/LATEX file prepared by the author.